Copper-Modified Zeolites and Silica for Conversion of Methane to Methanol

(article starts on next page)

Copper-Modified Zeolites and Silica for Conversion of Methane to Methanol

Xueting Wang [1], Natalia M. Martin [1], Johan Nilsson [1], Stefan Carlson [2], Johan Gustafson [3], Magnus Skoglundh [1] and Per-Anders Carlsson [1,*]

[1] Department of Chemistry and Chemical Engineering and Competence Centre for Catalysis, Chalmers University of Technology, 412 96 Gothenburg, Sweden; wangxu@chalmers.se (X.W.); natalia.martin@chalmers.se (N.M.M.); johan.nilsson@chalmers.se (J.N.); skoglund@chalmers.se (M.S.)
[2] MAX-IV Laboratory, Lund University, 221 00 Lund, Sweden; Stefan.Carlson@maxiv.lu.se
[3] Synchrotron Radiation Research, Lund University, 221 00 Lund, Sweden; johan.gustafson@sljus.lu.se
* Correspondence: per-anders.carlsson@chalmers.se; Tel.: +46-31-772-29-24

Abstract: Powder materials containing copper ions supported on ZSM-5 (Cu-Zeolite Socony Mobil-5) and SSZ-13 (Cu-Standard Oil synthesised zeolite-13), and predominantly CuO nanoparticles on amorphous SiO_2 were synthesised, characterised, wash-coated onto ceramic monoliths and, for the first time, compared as catalysts for direct conversion of methane to methanol (DCMM) at ambient pressure (1 atm) using O_2, N_2O and NO as oxidants. Methanol production was monitored and quantified using Fourier transform infrared spectroscopy. Methanol is formed over all monolith samples, though the formation is considerably higher for the copper-exchanged zeolites. Hence, copper ions are the main active sites for DCMM. The minor amount of methanol produced over the Cu/SiO_2 sample, however, suggests that zeolites are not the sole substrate that can host those active copper sites but also silica. Further, we present the first ambient pressure in situ infrared spectroscopic measurements revealing the formation and consumption of surface methoxy species, which are considered to be key intermediates in the DCMM reaction.

Keywords: methane partial oxidation; DCMM; supported copper ions; methoxy reaction intermediate species; in situ infrared spectroscopy; Cu-ZSM-5; Cu-SSZ-13; Cu/SiO_2

1. Introduction

Methane is the main component in natural gas, which attracts much attention as an abundant hydrocarbon source. In some regions, methane from renewable sources, biomethane or biogas, is becoming increasingly available as well. Renewable methane is beneficial as a green drop-in fuel or chemical feedstock that can increase industrial sustainability. To make use of methane in practice, however, it is often beneficial to convert it to a liquid compound as to increase the energy density, and facilitate distribution and storage. One strategy is to make methanol through partial oxidation of methane. Methanol is one of the industrial platform chemicals that also has the advantage of being biodegradable [1]. Present industrial methanol production from methane is an energy intensive process carried out in two steps: partial oxidation of methane to syngas (H_2 and CO) at elevated temperature followed by catalytic conversion of syngas to methanol at high pressure. The process infrastructure is costly and therefore direct conversion of methane to methanol (DCMM), preferably at low temperature, is an attractive alternative with lower energy loads and potentially cheaper installation costs. This solution, however, faces great challenges as both oxygen and methane are difficult to activate for catalytic partial oxidation, whereas methanol, once formed, may easily undergo further unwanted reactions that ruin the selectivity.

Methane monooxygenases (MMOs) are naturally occurring enzymes that have the ability to selectively oxidise methane to methanol under ambient conditions [2]. The active sites of MMOs are di-iron [3] or di-copper centres [4] in a peptide ligand environment. Inspired by the structure and chemical functionality of MMOs, copper exchanged zeolites are considered to be inorganic analogues to the MMOs with respect to functionality of the copper sites [5–7]. To produce methanol over copper zeolites, however, a quasi-catalytic reaction sequence is commonly employed. In this approach, an oxidative activation of the copper zeolite at high temperature is required before methane can be oxidised at a lower temperature. Subsequently, methanol is released from the catalyst upon extraction using water, ethanol or other solvents. Although this activation-reaction-extraction sequence can be avoided under some certain conditions [8,9], the catalytic activity requires to be significantly improved in order to be industrially relevant for DCMM.

With the aim to design more efficient catalysts based on copper zeolites, much efforts have been put into identifying the active sites for this reaction both experimentally [5–7,10–13] and theoretically [12–16]. Early studies suggest that the so-called α-oxygen in iron complexes (analogue to the di-iron centres in the α subunit of MMO [17]) is the key to methane activation [18]. Similarly, copper dimers have been proposed to be the necessary sites for hosting the reactive oxygens for methane activation [7,11]. Later studies, however, indicate that different types of copper species, i.e., copper monomers [16], copper dimers [6,10,12], copper trimers [13] or small copper clusters [19] in zeolites, can catalyse the partial oxidation of methane to methanol. The variety of active copper species should in principle bring increased flexibility to the catalyst design as an advantage. It is, however, not clear if the requirement for active copper sites can be generalised and applied more broadly for catalyst synthesis, i.e., zeolite-free systems. Therefore, it is of great interest to comparatively investigate materials containing different types of copper species. Moreover, unlike many other metal-zeolite reaction systems, no reaction intermediates, presumably such as surface-bound methyl or methoxy groups [20], have been directly observed for copper-modified small-pore zeolites under DCMM reaction conditions.

In the present work, we investigate materials containing copper ions supported on ZSM-5 (Cu-Zeolite Socony Mobil-5 [21]) and SSZ-13 (Cu-Standard Oil synthesised zeolite-13 [22]), as well as predominantly CuO nanoparticles on amorphous SiO_2, for direct oxidation of methane to methanol and use in situ infrared spectroscopy to monitor formation/consumption of surface species that play a role in the methanol formation. Methanol production over Cu-zeolites and Cu/SiO_2 is detected over coated monolith samples for the first time. We report that DCMM occurs over copper ions and that these copper species exist on silica but are more abundant in zeolite structures. We present—under ambient pressure—the formation/consumption of mechanistically important methoxy species over Cu-ZSM-5, Cu-SSZ-13 and Cu/SiO_2 during DCMM.

2. Results and Discussion

2.1. Methanol Production

Figure 1 presents the amount of produced methanol over the Cu-ZSM-5, Cu-SSZ-13 and Cu/SiO_2 sample. As can be seen in the figure, methanol is produced over all samples during the extraction step. Methanol production, however, for Cu-ZSM-5 (regardless of oxidant) and Cu-SSZ-13 (O_2 or N_2O) is clearly higher than that for Cu/SiO_2 or H-ZSM-5 (not shown), which is negligible. Interestingly, the use of different oxidants for the activation step results in similar amounts of formed methanol during extraction for the Cu-ZSM-5 sample whereas for the Cu-SSZ-13 sample, the methanol formation is clearly dependent on the oxidant. For Cu-ZSM-5, DCMM reaction has been correlated (only) with the mono(μ-oxo)dicupric site as characterised by the absorption band at 22,700 cm^{-1} in UV–vis spectrum [6,10]. Thus, it seems from the present results that this site can be activated by different oxidants. On the contrary, multiple absorption features in the UV–vis [9,23] and Raman [24,25] spectra have been reported for O_2/N_2O activated Cu-SSZ-13, which is indicative of the presence of various

Cu species active for DCMM. Moreover, the observed UV–vis bands after O_2 and N_2O activation [9] differs, suggesting that each oxidant activates distinct Cu species. This may be the reason for the different amounts of formed methanol observed here when using O_2 or N_2O.
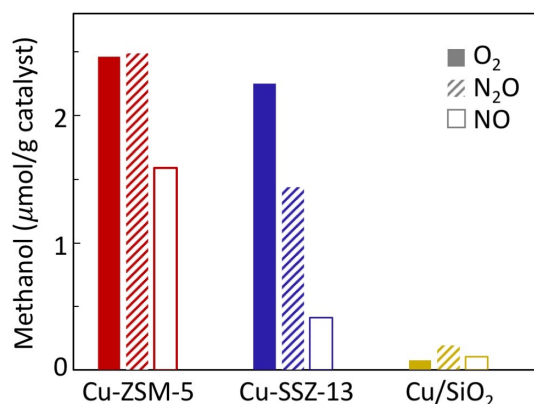

Figure 1. Methanol production over Cu-ZSM-5, Cu-SSZ-13 and Cu/SiO_2 at 1 atm using O_2, N_2O or NO as oxidants.

2.2. Catalyst Characterisation

In Figure 2a, the XANES spectra of Cu-ZSM-5, Cu-SSZ-13 and Cu foil at the Cu K-edge are shown. The spectra of Cu-ZSM-5 and Cu-SSZ-13 overlap with each other. No obvious pre-edge peak for Cu(I) (well defined peak at 8982–8984 eV [26,27]) or pre-edge shoulder for metallic Cu (Figure 2a, black spectrum) can be observed. Both spectra present a sharp absorption at about 8995–8998 eV. This is due to the 1*s*-to-4*p* electronic transition of Cu(II) species [26], indicating that the dominating oxidation state of the copper species is Cu(II) in both copper zeolite samples. The featureless pre-edge, however, signifies the absence of CuO species (weak absorption at about 8976–8979 eV and a shoulder at about 8985–8988 eV [27]), indicating that the Cu-ZSM-5 and Cu-SSZ-13 samples do not contain detectable amounts of large CuO domains. The spectrum of the Cu foil presents an evident pre-edge feature around 8983 eV with resonance features above the edge that are clearly different from the spectra of Cu-ZSM-5 and Cu-SSZ-13. Figure 2b presents the Fourier transforms of the Cu K-edge EXAFS spectra of the Cu-ZSM-5 and the Cu-SSZ-13 sample as well as that of the reference compounds: Cu, Cu_2O and CuO. Both Cu-ZSM-5 and Cu-SSZ-13 sample exhibit an intensive peak at around 1.5 Å, associated with the neighbouring O atoms. The absence of peaks at the range of 2.5–3 Å, suggesting the lack of neighbouring Cu atoms, indicating that isolated Cu ions are the dominant Cu species in these samples. Moreover, the calculated Cu/Al ratio of the Cu-ZSM-5 and Cu-SSZ-13 sample is 0.38 and 0.14 respectively. At such ion-exchange levels, Cu dispersion is 100% in ZSM-5 [28] and the Cu species in SSZ-13 are dominantly monomers [29].

In Figure 2c, the XRD patterns of the Cu-ZSM-5, Cu-SSZ-13 and Cu/SiO_2 samples are shown. The XRD patterns of the Cu-ZSM-5 and Cu-SSZ-13 samples exhibit only characteristic peaks of the respective zeolite structure [30] (the XRD patterns of the parent zeolites are presented in the Supplementary Materials Figure S1), while no reflections of crystalline Cu species are visible. This suggests that the Cu species in these samples are smaller than 2–3 nm. Additional CO and NO adsorption experiments shown in the Supplementary Materials Figure S2 confirm the presence of cationic copper species in both the Cu-ZSM-5 and the Cu-SSZ-13 sample. For the diffractogram of the Cu/SiO_2 sample, reflections characteristic of crystalline CuO are evident, indicating the existence of CuO particles. The mean crystalite size of CuO is 28.3 nm calculated with Scherrer's equation [31] (shape factor 0.89) using the full width at half-maximum (FWHM) of the characteristic peak of CuO (111) ($2\theta = 38.92°$). The CO and NO adsorption spectra shown in Figure S2 (Supplementary Materials), however, indicate the presence of cationic copper species in small amount on the Cu/SiO_2 sample.

The results from XRD and CO/NO adsorption experiments picture the Cu/SiO_2 sample dominated with CuO nanoparticles accompanied by small amount of cationic Cu species.
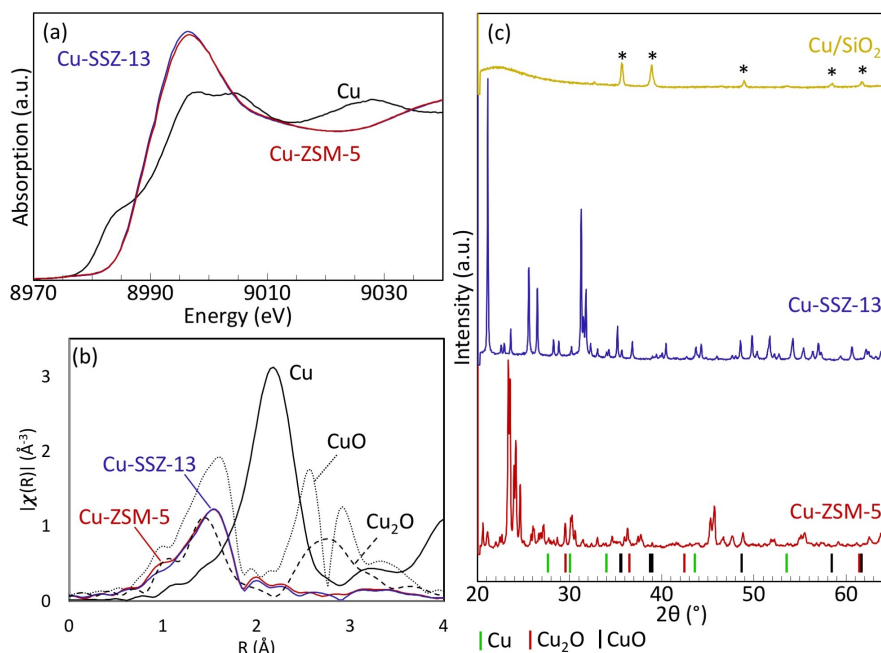

Figure 2. (**a**) XANES spectra of the Cu-ZSM-5 (red), Cu-SSZ-13 (blue) and Cu foil (black), as reference; (**b**) magnitude of Fourier transformed EXAFS spectra (k-weight = 2) of Cu-ZSM-5 (red), Cu-SSZ-13 (blue), Cu foil (solid black line), Cu_2O (dashed black line, the Farrel Lytle database #cu2o.514) [32] and CuO (dotted black line, the Farrel Lytle database #cuoxop.027) [32]; (**c**) XRD patterns of the Cu-ZSM-5, Cu-SSZ-13 and Cu/SiO_2 samples; the characteristic reflections of the CuO crystalline structure are denoted with asterisks (*); the coloured bars at the bottom representing the reflections of Cu (green, SpringerMaterials sd_1928261), Cu_2O (red, SpringerMaterials sd_1928262) and CuO (black, the American Mineralogist Crystal Structure Database #0018812).

2.3. In Situ IR Study of Methane Oxidation and Water Extraction

Figure 3 presents the IR spectra during methane oxidation (solid lines) and water extraction (dashed lines) for all three samples. The presented spectra are focused on the C-H and C=O stretching vibration regions. Beside the gas phase methane (3017 cm^{-1}) [33], C-H stretching bands originated from adsorbed species are visible between 2800 and 3050 cm^{-1} for all three samples after methane oxidation. For the Cu-ZSM-5 sample, absorption bands of methoxy groups adsorbed on Brønsted acid sites (2978 cm^{-1}) [34–37], formate on Cu (2906 cm^{-1}) [37] and CO on Cu (2157 cm^{-1}) [38] appear after 2 h exposure to methane. The evolution of these bands indicates that methane is oxidised and the oxidation products are stable on the sample surface. The low intensity of the bands, however, suggest low concentration of the adsorbed oxidised species. With longer exposure time to methane, CO accumulates on the copper species while the amount of C-H containing species remains fairly constant. Similar features at the C-H stretching vibrational region in IR spectra has been previously observed over Cu-MOR upon exposure to methane at higher pressure [39]. After exposing the Cu-SSZ-13 and Cu/SiO_2 samples to methane for 2 h, a peak at 2968 cm^{-1} arises for both samples while the peak at 2911 cm^{-1} is visible only for Cu-SSZ-13. Though it is expected that these bands are associated with adsorbed species originated from methane, the exact assignments are not apparent. Bands at wavenumbers close to 2968 cm^{-1} (ν_3 mode) and 2911 cm^{-1} (ν_1 mode) have been observed during methane adsorption on silica [40,41] and zeolites [41–43] due to dissosiative adsorption of methane. Moreover, methoxy groups adsorbed on Brønsted acid sites (2968 cm^{-1}), extra framework Al (2978 cm^{-1}) and Si (2957 cm^{-1}) may contribute to the band at 2968 cm^{-1} for the Cu-SSZ-13 sample. It is clear that methane can adsorb dissociatively on the Cu-SSZ-13 and Cu/SiO_2 samples at 250 °C.

The absence of features in the C=O stretching vibration region, however, suggests that the ability of these samples to catalyse further oxidation of methane at 250 °C is negligible. Interestingly, CO forms during methane oxidation over the Cu sites in the Cu-ZSM-5 sample but not over the Cu-SSZ-13 sample. This can be due to the higher concentration of copper in the Cu-ZSM-5 sample, which is more than twice the amount of copper in the Cu-SSZ-13 sample. Moreover, a previous study has shown that Cu-SSZ-13 exhibits much higher methanol selectivity and lower CO or CO_2 selectivity during catalytic methane oxidation compared to Cu-ZSM-5 with similar Cu loading [9]. It has been discovered that zeolites with the majority of the adsorption sites in 8-membered ring (MR) rather than in 6, 10 or 12 MRs (e.g., SSZ-13) can host higher concentrations of Cu species active for methanol formation [24,44]. Therefore, the lack of CO formation in the Cu-SSZ-13 sample can be a combination of low Cu loading that results in copper sites predominantly favouring formation of methanol rather than CO. Furthermore, the Cu species in Cu-SSZ-13 has been shown to be considerably more stable than Cu-ZSM-5 for which copper species may agglomerate to larger Cu-oxo clusters that promote CO formation [45]. After water extraction (dashed lines in Figure 3), though most bands remain for the Cu-ZSM-5 and Cu-SSZ-13 samples, the bands related to methoxy on Brønsted acid sites (2978 cm^{-1}), formate (2906 cm^{-1}) and CO (2157 cm^{-1}) decrease in intensity for Cu-ZSM-5, while the intensity of band at 2968 cm^{-1} decreases for Cu-SSZ-13. It is anticipated that the methoxy species adsorbed on the Cu-ZSM-5 and Cu-SSZ-13 samples react with water and desorb from the sample surface as methanol, leaving other more strongly adsorbed species, presumably methyl. For the Cu/SiO_2 sample, however, no obvious decrease in intensity is observed for the band at 2968 cm^{-1}, which suggest that a trivial amount of methanol is produced during water extraction. These speculations are further supported by the activity studies discussed above.
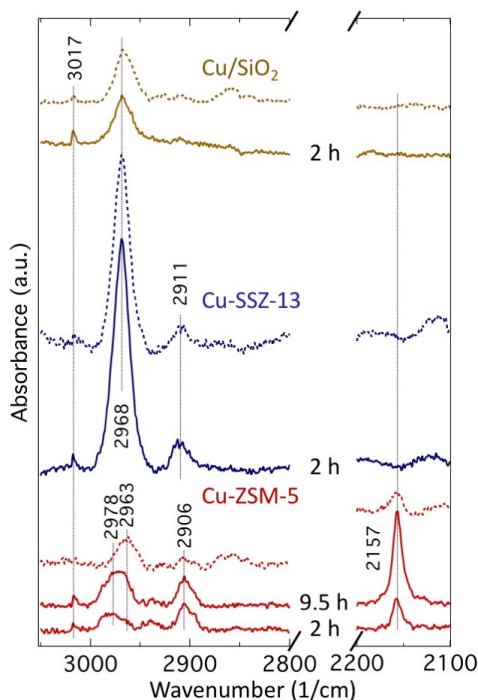

Figure 3. IR spectra of the Cu-ZSM-5, Cu-SSZ-13 and Cu/SiO_2 sample exposed to methane (solid line marked with exposure time) and after water extraction for 10 min (dashed line) at 250 °C. The IR measurements were carried out at 1 atm.

2.4. Concluding Discussion

In summary, X-ray-based characterisation and infrared analysis of CO/NO adsorption show that the prepared Cu-ZSM-5 and Cu-SSZ-13 samples contain cationic copper species. On the contrary, the Cu/SiO_2 sample is dominated by CuO particle sites and silica sites with the presence of cationic

copper species in small amount. Methanol production is, to our knowledge for the first time, detected over the Cu-ZSM-5, Cu-SSZ-13 and Cu/SiO$_2$ monolith catalysts. The choice of sample form is different from that of the previous literatures which were conducted over powder or pellet samples. The monolith samples allow sufficient flow without detrimental pressure drop as to achieve reasonable time resolution in the FTIR gas phase analysis. The in situ infrared measurements reveal the formation of surface bound methoxy species as a likely important reaction intermediate during methane oxidation as well as the consumption of these methoxy species during water extraction, which is considerably more pronounced for the zeolitic systems. Hence, the higher methanol formation from Cu-ZSM-5 and Cu-SSZ-13 compared with Cu/SiO$_2$ can be attributed to the isolated Cu ions in consistence with previous suggestions [5,10,11,14–16,46]. Notably, here, the minor amount of formed methanol (3.5–6.4 μmol/g Cu) over the Cu/SiO$_2$ sample regardless of oxidant is an interesting observation. Although the Cu/SiO$_2$ sample contains CuO particles as observed by XRD, one can not neglect the presence of copper ions possibly in the form of monomers, dimers or small ensembles. These ions are likely responsible for the formation of methanol in this case. The reason for the low amount of formed methanol may in this case be due to the low abundance of ionic copper species, or that the ionic copper species co-exist with larger CuO particles, which promote total oxidation such that the selectivity towards methanol becomes low. This speculation in turn suggests that the zeolite structure is not the only type of substrate that can host copper species active for DCMM as generally discussed hitherto. One may thus envisage that the choice of support may be more flexible than previously discussed such that catalyst design should primarily target the creation of small ensembles of copper ions, however, not necessarily contained in zeolites. In fact, low methanol production (less than 1 μmol/g Cu) has been previously observed over alumina containing Cu/silica system [7]. A very recent study also described the formation of active Cu species when proper conditions were used [47]. This is encouraging as for example ZSM-5 is a dehydration catalyst that is used to convert methanol to dimethyl ether (DME) in the well known methanol to gasoline (MTG) process [48] and therefore not the ideal substrate when striving for high methanol production. In fact, when much methanol is adsorbed, DME formation is evident already at 175 °C [37], which is in the target temperature range suitable for DCMM. At present, however, the low methanol formation presented here and elsewhere allows for using ZSM-5 without any particular issues concerning DME formation.

3. Experimental Section

3.1. Catalyst Preparation

For this study, Cu-zeolite samples, Cu-ZSM-5 and Cu-SSZ-13, were prepared using aqueous ion-exchange [6]. The ion-exchange was carried out by mixing aqueous solutions of Cu(NO$_3$)$_2$ (0.1 M, 100 mL/g zeolite) with H-ZSM-5 (Si/Al = 13.5, Akzo Nobel, Amsterdam, The Netherlands) or H-SSZ-13 (Si/Al = 10, synthesised according to the method described by Shishkin et al. [49,50]) at room temperature for 24 h. The pH of the solution was kept at around 4.5 by addition of ammonia solution when necessary. After ion-exchange the slurry was filtered and the solid fraction was washed with Milli-Q water (18 MΩ·cm) and then dried at 120 °C in air overnight. Inductively coupled plasma-sector field mass spectrometry (ICP-SFMS) gives a Cu loading of 2.8 wt.% for the Cu-ZSM-5 sample and 1.3 wt.% for the Cu-SSZ-13 sample. The Cu/SiO$_2$ sample was prepared using incipient wetness impregnation where an aqueous solution of Cu(NO$_3$)$_2$·5H$_2$O (Sigma-Aldrich, St. Louis, MO, USA, ACS reagent, 0.29 M, 1.66 mL/g silica) was slowly added to the silica support (Akzo Nobel, Kromasil, 200 Å, 5 μm). The mixture was then instantly frozen by liquid nitrogen and freeze-dried over night before calcined in air at 350 °C for 3 h. The Cu loading was 3.0 wt.% for the Cu/SiO$_2$ sample. Part of the Cu-ZSM-5, Cu-SSZ-13 and Cu/SiO$_2$ powder samples were used for wash-coating cordierite monolith substrates (Corning, New York, NY, USA, 400 cpsi, L = 15 mm, Ø = 13 mm). For each catalyst sample, a slurry was prepared by mixing the powder catalyst sample with a binder (Sasol, Sandton, South Africa, Disperal P2) at a weight ratio of 80:20 in Milli-Q water. The calcined monolith substrates

were coated with thin layers of the wash-coat until the added solid material on each substrate reached 0.2 g. The monolith samples were finally calcined at 600 °C for 3 h.

3.2. Activity Test

Catalytic activity tests of the prepared monolith samples were carried out using a chemical flow reactor system equipped with an FTIR analyser (MKS 2030 FTIR spectrometer) for continuous analysis of the effluent stream. The flow reactor consists of a horizontal quartz tube surrounded with an insulated metal coil for resistive heating. The catalyst temperature is measured by a type K thermocouple and controlled with a PID regulator (Eurotherm, Worthing, UK). The feed gas system consists of separate mass flow controllers (Bronkhorst Hi-Tech, Ruurlo, Netherlands, Low-ΔP-Flow) for the different gases and a water vapour generator that catalytically produces ultra-pure water vapour from high-purity H_2 and O_2 gases [51]. The activity test for direct conversion of methane to methanol was carried out through an activation-reaction-extraction sequential approach at 1 atm. In this approach, the samples were first activated at 550 °C with the oxidant (20% vol O_2, 300 vol ppm N_2O or 0.1% vol NO) for one hour before exposure to 2% vol CH_4 at 150 °C for one hour. The products were then extracted with water vapour (4% vol for Cu-SSZ-13 and Cu/SiO_2, and 8% vol for Cu-ZSM-5) at 150 °C. The methanol production was acquired by applying a peak area integration of the methanol concentration as measured by the gas phase FTIR analyser during the water extraction step. During this phase methanol was the main product together with a minor amount of CO_2.

3.3. Characterisation

To correlate the methanol formation to relevant materials properties, X-ray based characterisation was carried out. The local environment of copper was characterised by X-ray absorption spectroscopy (XAS) at beamline I811 at the MAX IV Laboratory, Lund, Sweden. Spectra were recorded at the Cu K-edge (8979 eV) in fluorescence mode. The photon energy was calibrated using a Cu foil measured simultaneously with the sample. The X-ray absorption near edge structure (XANES) spectra were processed using the Athena software [52].

The crystal phases of the samples were determined by X-ray diffraction (XRD) using a Bruker XRD D8 Advance instrument with monochromatic CuK$_{\alpha 1}$ radiation scanning 2θ from 20 to 60° (step size 0.029°, dwell time 1 s).

The in situ infrared spectroscopic measurements were carried out in diffuse reflectance mode using a VERTEX 70 spectrometer (Bruker) equipped with a liquid nitrogen cooled mercury cadmium telluride detector with the band width 600–12,000 cm^{-1}, a Praying Mantis^{TM} diffuse reflectance accessory and a high-temperature stainless steel reaction chamber (Harrick Scientific Products Inc., New York, NY, USA). All spectra were measured between 900 and 4000 cm^{-1} with a spectral resolution of 1 cm^{-1}. The instrumental aperture was 3 mm wide with a four times sensitivity gain. About 85 μL sample was loaded into the reaction chamber. Methane oxidation experiments were carried out for all three samples, i.e., Cu-ZSM-5, Cu-SSZ-13 and Cu/SiO_2, at 1 atm. After pre-treatment with 500 vol ppm N_2O at 550 °C for one hour, 2% vol of methane was fed to the sample at 250 °C. Finally, the extraction step was carried out with 0.25 g/h water in Ar at 250 °C. All spectra were recorded in pure Ar. The backgrounds were taken in Ar at 250 °C for each sample after the sample pre-treatment. Baseline subtraction is carried out for all spectra using the Igor Pro software. For the IR study, the set reaction temperature is 250 °C instead of 150 °C, which is used in the flow reactor. The reason for using this set temperature is that the cell design causes temperature gradients in the sample bed, such that the temperature in the volume probed by IR is considerably lower than the set temperature [53]. The set reaction temperature used in the present study results in similar temperatures for the flow-reactor experiments and the IR measurements.

4. Conclusions

For copper-based catalytic materials, the direct conversion of methane to methanol requires ionic copper sites. Such sites are abundant in copper-exchanged zeolites, i.e., Cu-ZSM-5 and Cu-SSZ-13, which show clear methanol formation, but seem to exist also in Cu/SiO_2, although to a minor extent reflected by the minor methanol formation. In situ infrared spectroscopic measurements reveal that on these sites, the methanol formation proceeds through the formation/consumption of surface methoxy species, which are considered to be important intermediates in the direct conversion of methane to methanol.

Author Contributions: X.W. carried out all experiments and is main responsible for preparing the paper; N.M.M. assisted in the XAS measurments; J.N. assisted in the XAS measurments; S.C. assisted in the set-up and operation of the XAS beam line; J.G. interpreted the XRD results; M.S. guided and discussed the experiments; P.-A.C. is principle investigator who conceived the idea and supervised the work.

Conflicts of Interest: The authors declare no conflict of interest.

References

1. Goldberg, I.; Rokem, J.S. *Biology of Methylotrophs*; Butterworth-Heinemann: Stoneham, MA, USA, 1991; p. 3.
2. Woodland, M.P.; Dalton, H. Purification of Component A of the Soluble Methane Monooxygenase of *Methylococcus capsulatus* (Bath) by High-pressure Gel-permeation Chromatography. *Anal. Biochem.* **1984**, *139*, 459–462. [CrossRef]
3. Ji, Y.; Mao, G.; Wang, Y.; Bartlam, M. Structural Insights into Diversity and N-alkane Biodegradation Mechanisms of Alkane Hydroxylases. *Front. Microbiol.* **2013**, *4*, 1–13. [CrossRef] [PubMed]
4. Citek, C.; Gary, J.B.; Wasinger, E.C.; Stack, T.D. Chemical Plausibility of Cu-(III) with Biological Ligation in pMMO. *J. Am. Chem. Soc.* **2015**, *137*, 6991–6994. [CrossRef] [PubMed]
5. Vanelderen, P.; Hadt, R.G.; Smeets, P.J.; Solomon, E.I.; Schoonheydt, R.A.; Sels, B.F. Cu-ZSM-5: A Biomimetic Inorganic Model for Methane Oxidation. *J. Catal.* **2011**, *284*, 157–164. [CrossRef] [PubMed]
6. Beznis, N.V.; Weckhuysen, B.M.; Bitter, J.H. Cu-ZSM-5 Zeolites for the Formation of Methanol from Methane and Oxygen: Probing the Active Sites and Spectator Species. *Catal. Lett.* **2010**, *138*, 14–22. [CrossRef]
7. Groothaert, M.H.; Smeets, P.J.; Sels, B.F.; Jacobs, P.A.; Schoonheydt, R.A. Selective Oxidation of Methane by the Bis(μ-oxo)dicopper Core Stabilized on ZSM-5 and Mordenite Zeolites. *J. Am. Chem. Soc.* **2005**, *127*, 1394–1395. [CrossRef] [PubMed]
8. Narsimhan, K.; Iyoki, K.; Dinh, K.; Román-Leshkov, Y. Catalytic Oxidation of Methane into Methanol over Copper-Exchanged Zeolites with Oxygen at Low Temperature. *ACS Cent. Sci.* **2016**, *2*, 424–429. [CrossRef] [PubMed]
9. Ipek, B.; Lobo, R.F. Catalytic Conversion of Methane to Methanol on Cu-SSZ-13 Using N_2O as Oxidant. *Chem. Commun.* **2016**, *52*, 13401–13404. [CrossRef] [PubMed]
10. Woertink, J.S.; Smeets, P.J.; Groothaert, M.H.; Vance, M.A.; Sels, B.F.; Schoonheydt, R.A.; Solomon, E.I. A $[Cu_2O]^{2+}$ Core in Cu-ZSM-5, the Active Site in the Oxidation of Methane to Methanol. *Proc. Natl. Acad. Sci. USA* **2009**, *106*, 18908–18913. [CrossRef] [PubMed]

11. Smeets, P.J.; Groothaert, M.H.; Schoonheydt, R.A. Cu Based Zeolites: A UV-vis Study of the Active Site in the Selective Methane Oxidation at Low Temperatures. *Catal. Today* **2005**, *110*, 303–309. [CrossRef]

12. Alayon, E.M.C.; Nachtegaal, M.; Bodi, A.; Ranocchiari, M.; van Bokhoven, J.A. Bis(μ-oxo) Versus Mono(μ-oxo)dicopper Cores in a Zeolite for Converting Methane to Methanol: An In Situ XAS and DFT Investigation. *Phys. Chem. Chem. Phys.* **2015**, *17*, 7681–7693. [CrossRef] [PubMed]

13. Grundner, S.; Markovits, M.A.C.; Li, G.; Tromp, M.; Pidko, E.A.; Hensen, E.J.M.; Jentys, A.; Sanchez-Sanchez, M.; Lercher, J.A. Single-site Trinuclear Copper Oxygen Clusters in Mordenite for Selective Conversion of Methane to Methanol. *Nat. Commun.* **2015**, *6*, 1–9. [CrossRef] [PubMed]

14. Tsai, M.L.; Hadt, R.G.; Vanelderen, P.; Sels, B.F.; Schoonheydt, R.A.; Solomon, E.I. $[Cu_2O]^{2+}$ Active Site Formation in Cu-ZSM-5: Geometric and Electronic Structure Requirements for N_2O Activation. *J. Am. Chem. Soc.* **2014**, *136*, 3522–3529. [CrossRef] [PubMed]

15. Li, G.; Vassilev, P.; Sanchez-Sanchez, M.; Lercher, J.A.; Hensen, E.J.M.; Pidko, E.A. Stability and Reactivity of Copper Oxo-clusters in ZSM-5 Zeolite for Selective Methane Oxidation to Methanol. *J. Catal.* **2016**, *338*, 305–312. [CrossRef]

16. Kulkarni, A.R.; Zhao, Z.J.; Siahrostami, S.; Nørskov, J.K.; Studt, F. Monocopper Active Site for Partial Methane Oxidation in Cu-Exchanged 8MR Zeolites. *ACS Catal.* **2016**, *10*, 6531–6536. [CrossRef]

17. Feig, A.L.; Lippard, S.J. Reactions of Non-Heme Iron(II) Centers with Dioxygen in Biology and Chemistry. *Chem. Rev.* **1994**, *94*, 759–805. [CrossRef]

18. Dubkov, K.A.; Sobolev, V.I.; Talsi, E.P.; Rodkin, M.A.; Watkins, N.H.; Shteinman, A.A.; Panov, G.I. Kinetic Isotope Effects and Mechanism of Biomimetic Oxidation of Methane and Benzene on FeZSM-5 Zeolite. *J. Mol. Catal. A Chem.* **1997**, *123*, 155–161. [CrossRef]

19. Tomkins, P.; Mansouri, A.; Bozbag, S.E.; Krumeich, F.; Park, M.B.; Alayon, E.M.; Ranocchiari, M.; van Bokhoven, J.A. Isothermal Cyclic Conversion of Methane into Methanol over Copper-Exchanged Zeolite at Low Temperature. *Angew. Chem. Int. Ed.* **2016**, *55*, 5467–5471. [CrossRef] [PubMed]

20. Arvidsson, A.A.; Zhdanov, V.P.; Carlsson, P.A.; Grönbeck, H.; Hellman, A. Metal Dimer Sites in ZSM-5 Zeolite for Methane-to-Methanol Conversion from First-Principles Kinetic Modelling: Is the $[Cu–O–Cu]^{2+}$ Motif Relevant for Ni, Co, Fe, Ag, and Au? *Catal. Sci. Technol.* **2017**, *7*, 1470–1477. [CrossRef]

21. Argauer, R.J.; Landolt, G.R. Crystalline Zeolite ZSM-5 and Method of Preparing the Same. U.S. Patent 3,702,886, 14 November 1972.

22. Hadjiivanov, K. *Advances in Catalysis*; Academic Press: New York, NY, USA, 2014; Volume 57, p. 101.

23. Oord, R.; Schmidt, J.E.; Weckhuysen, B.M. Methane-to-methanol Conversion over Zeolite Cu-SSZ-13, and Its Comparison with the Selective Catalytic Reduction of NO_x with NH_3. *Catal. Sci. Technol.* **2018**, *8*, 1028–1038. [CrossRef]

24. Ipek, B.; Wulfers, M.J.; Kim, H.; Göltl, F.; Hermans, I.; Smith, J.P.; Booksh, K.S.; Brown, C.M.; Lobo, R.F. Formation of $[Cu_2O_2]^{2+}$ and $[Cu_2O]^{2+}$ toward C-H Bond Activation in Cu-SSZ-13 and Cu-SSZ-39. *ACS Catal.* **2017**, *7*, 4291–4303. [CrossRef]

25. Pappas, D.K.; Borfecchia, E.; Dyballa, M.; Pankin, I.A.; Lomachenko, K.A.; Martini, A.; Signorile, M.; Teketel, S.; Arstad, B.; Berlier, G.; et al. Methane to Methanol: Structure-Activity Relationships for Cu-CHA. *J. Am. Chem. Soc.* **2017**, *139*, 14961–14975. [CrossRef] [PubMed]

26. Lamberti, C.; Bordiga, S.; Salvalaggio, M.; Spoto, G.; Zecchina, A. XAFS, IR, and UV-Vis Study of the Cu^I Environment in Cu^I-ZSM-5. *J. Phys. Chem. B* **1997**, *101*, 344–360. [CrossRef]

27. Groothaert, M.H.; Bokhoven, J.A.V.; Battiston, A.A.; Weckhuysen, B.M.; Schoonheydt, R.A. Bis(μ-oxo)dicopper in Cu-ZSM-5 and Its Role in the Decomposition of NO: A Combined in Situ XAFS, UV-Vis-Near-IR, and Kinetic Study. *J. Am. Chem. Soc.* **2002**, *125*, 7629–7640. [CrossRef] [PubMed]

28. de Carvalho, M.C.A.; Passos, F.B.; Schmal, M. Quantification of metallic area of high dispersed copper on ZSM-5 catalyst by TPD of H_2. *Catal. Commun.* **2002**, *3*, 503–509. [CrossRef]

29. Martini, A.; Borfecchia, E.; Lomachenko, K.A.; Pankin, I.A.; Negri, C.; Berlier, G.; Beato, P.; Falsig, H.; Bordiga, S.; Lamberti, C. Composition-driven Cu-speciation and reducibility in Cu-CHA zeolite catalysts: A multivariate XAS/FTIR approach to complexity. *Chem. Sci.* **2017**, *8*, 6836–6851. [CrossRef] [PubMed]

30. International Zeolite Association Webpage. Available online: http://europe.izastructure.org (accessed on 14 March 2017).

31. Scherrer, P. Bestimmung der Größe und der Inneren Struktur von Kolloidteilchen Mittels Röntgenstrahlen. *Nachr. Ges. Wiss. Göttingen Math. Phys. Klasse* **1918**, *3*, 98–100.

32. The Farrel Lytle Database. Available online: http://ixs.csrri.iit.edu/database/data/Farrel_Lytle_data/ (accessed on 18 May 2017).

33. Manzanares, C.; Brock, A.; Peng, J.; Blunt, V.M. Vibrational Spectroscopy of C-H Bonds of Methane and Tetramethylsilane in Liquid Argon Solutions. *Chem. Phys. Lett.* **1993**, *207*, 159–166. [CrossRef]

34. Kung, M.C.; Lin, S.S.Y.; Kung, H.H. In situ Infrared Spectroscopic Study of CH_4 Oxidation Over Co-ZSM-5. *Top. Catal.* **2012**, *55*, 108–115. [CrossRef]

35. Wood, B.R.; Reimer, J.A.; Bell, A.T.; Janicke, M.T.; Ott, K.C. Methanol Formation on Fe/Al-MFI via the Oxidation of Methane by Nitrous Oxide. *J. Catal.* **2004**, *225*, 300–306. [CrossRef]

36. Campbell, S.M.; Jiang, X.Z.; Howe, R.F. Methanol to Hydrocarbons: Spectroscopic Studies and the Significance of Extra-Framework Aluminium. *Microporous Mesoporous Mater.* **1999**, *29*, 91–108. [CrossRef]

37. Wang, X.; Arvidsson, A.A.; Cichocka, M.O.; Zou, X.; Martin, N.M.; Nilsson, J.; Carlson, S.; Gustafson, J.; Skoglundh, M.; Hellman, A.; et al. Methanol Desorption from Cu-ZSM-5 Studied by In Situ Infrared Spectroscopy and First-Principles Calculations. *J. Phys. Chem. C* **2017**, *121*, 27389–27398. [CrossRef]

38. Hadjiivanov, K.I.; Kantcheva, M.M.; Klissurski, D.G. IR Study of CO Adsorption on Cu-ZSM-5 and CuO/SiO_2 Catalysts: δ and π Components of the Cu^+-CO Bond. *J. Chem. Soc. Faraday Trans.* **1996**, *92*, 4595–4600. [CrossRef]

39. Sushkevich, V.L.; Palagin, D.; Ranocchiari, M.; van Bokhoven, J.A. Selective anaerobic oxidation of methane enables direct synthesis of methanol. *Science* **2017**, *356*, 523–527. [CrossRef] [PubMed]

40. Permenov, D.G.; Radzig, V.A. Mechanisms of Heterogeneous Processes in the System SiO_2 + CH_4: I. Methane Chemisorption on a Reactive Silica Surface. *Kinet. Catal.* **2004**, *45*, 14–23. [CrossRef]

41. Chen, L.; Lin, L.; Xu, Z.; Zhang, T.; Liang, D. Interaction of Methane with Surfaces of Silica, Aluminas and HZSM-5 Zeolite. A Comparative FT-IR Study. *Catal. Lett.* **1995**, *35*, 245–258. [CrossRef]

42. Kazansky, V.B. State and Properties of Ion-exchanged Cations in Zeolites: 2. IR Spectra and Chemical Activation of Adsorbed Methane. *Kinet. Catal.* **2014**, *55*, 737–747. [CrossRef]

43. Kazanskii, V.; Serykh, A.; Bell, A. Diffuse-reflectance IR Spectra of Methane Adsorbed on NaZSM-5 and HZSM-5 zeolites. *Kinet. Catal.* **2002**, *43*, 419–426. [CrossRef]

44. Park, M.B.; Ahn, S.H.; Mansouri, A.; Ranocchiari, M.; van Bokhoven, J.A. Comparative Study of Diverse Copper Zeolites for the Conversion of Methane into Methanol. *ChemCatChem* **2017**, *9*, 3705–3713. [CrossRef]

45. Deka, U.; Lezcano-Gonzalez, I.; Weckhuysen, B.M.; Beale, A.M. Local Environment and Nature of Cu Active Sites in Zeolite-Based Catalysts for the Selective Catalytic Reduction of NO_x. *ACS Catal.* **2013**, *3*, 413–427. [CrossRef]

46. Yumura, T.; Hirose, Y.; Wakasugi, T.; Kuroda, Y.; Kobayashi, H. Roles of Water Molecules in Modulating the Reactivity of Dioxygen-Bound Cu-ZSM-5 toward Methane: A Theoretical Prediction. *ACS Catal.* **2016**, *6*, 2487–2495. [CrossRef]

47. Bozbag, S.E.; Sot, P.; Nachtegaal, M.; Ranocchiari, M.; van Bokhoven, J.A.; Mesters, C. Direct Stepwise Oxidation of Methane to Methanol over $Cu-SiO_2$. *ACS Catal.* **2018**, *8*, 5721–5731. [CrossRef]

48. Keil, F.J. Methanol-to-hydrocarbons: Process Technology. *Microporous Mesoporous Mater.* **1999**, *29*, 49–66. [CrossRef]

49. Shishkin, A.; Kannisto, H.; Carlsson, P.A.; Härelind, H.; Skoglundh, M. Synthesis and Functionalization of SSZ-13 as an NH_3-SCR Catalyst. *Catal. Sci. Technol.* **2014**, *4*, 3917–3926. [CrossRef]

50. Zones, S.I. Zeolite SSZ-13 and Its Method of Preparation. U.S. Patent 4,544,538, 1 October 1985.

51. Velin, P.; Stenman, U.; Skoglundh, M.; Carlsson, P.A. Portable Device for Generation of Ultra-pure Water Vapor Feeds. *Rev. Sci. Instrum.* **2017**, *88*, 115102. [CrossRef] [PubMed]

52. Ravel, B.; Newville, M. ATHENA, ARTEMIS, HEPHAESTUS: Data Analysis for X-ray Absorption Spectroscopy Using IFEFFIT. *J. Synchrotron Rad.* **2005**, *12*, 537–541. [CrossRef] [PubMed]

53. Li, H.; Rivallan, M.; Thibault-Starzyk, F.; Travert, A.; Meunier, F.C. Effective Bulk and Surface Temperatures of the Catalyst Bed of FT-IR Cells Used for in situ and operando Studies. *Phys. Chem. Chem. Phys.* **2013**, *15*, 7321–7327. [CrossRef] [PubMed]